J Fail. Anal. and Preven. (2019) 19:1093–1104
https://doi.org/10.1007/s11668-019-00699-7

TECHNICAL ARTICLE—PEER-REVIEWED

Study on Vibration Characteristics of Fracturing Piping in Pump-Starting and Pump-Stopping Water Hammer

Yinping Cao · Yihua Dou · Yuxi Huang · Jiarui Cheng

Submitted: 17 December 2018 / in revised form: 18 July 2019 / Published online: 22 August 2019

Abstract In pump-starting and pump-stopping, because of the rapid change in fracturing fluid, the piping is subjected to water hammer effect. Water hammer effect results in severe vibration, which may damage the pipe or cause sealing failure of connections. To quantitatively analyze the water hammer effect and vibration characteristics in pump-starting and pump-stopping, the characterized lines method was adopted to analyze the velocities and dynamic pressures of fracturing fluid, as well as the axial velocities and additional stresses of piping at different depths. It shows that in pump-starting, the velocities and dynamic pressures of fracturing fluid as well as the axial velocities and additional stresses of piping increase greatly with increased flow rate of fracturing fluid. Meanwhile, the fluctuations of dynamic pressure and the axial velocities of piping decrease with increased depth. In the pump-stopping process, the shorter the pumping-stop time is, the higher the dynamic pressure of the fracturing fluid and the greater the axial velocity of the pipe. It is easier to damage the pipe in pump-stopping compared to pump-starting. The study provides a guidance of the flow rate of fracturing fluid, pump-starting time, and pump-stopping time to ensure safe fracturing.

Keywords Water hammer · Vibration · Pump-starting · Pump-stopping · Fracturing fluid · Piping

Y. Cao (✉) · Y. Dou · Y. Huang · J. Cheng
Mechanical Engineering College, Xi'an Shiyou University, Xi'an 710065, China
e-mail: caoyinping029@163.com

Y. Dou
e-mail: yhdou029@163.com

List of Symbols

x	Axial direction of piping (m)
ρ	Density of fracturing fluid (kg/m^3)
v	Velocity of fracturing fluid (m/s)
c	Propagation velocity of pressure wave (m/s)
λ	Friction resistance coefficient (dimensionless)
d	Inner diameter of piping (m)
Q_0	Initial flow rate, zero (m^3/s)
A	Coefficient of increased flow rate (dimensionless)
t	Pump-starting time (s)
τ	Ratio of a certain time and total pump-stopping time (dimensionless)
p_0	Initial pump pressure (Pa)
$v_{\max}$	The maximum velocity of fracturing fluid (m/s)
T	Total pump-stop time (s)
n	Coefficient in pump-stopping process (dimensionless)

Introduction

With the increasing difficulty of oil and gas production, conventional methods are not suitable for HPHT (high temperature and high pressure) wells and unconventional oil and gas wells. For these oil and gas wells, fracturing or even SRV (stimulated reservoir volume) fracturing is often adopted to increase production. Fracturing is to artificially make fractures, thus improving the flow environment of oil and gas in reservoirs. Fracturing fluid is the working fluid used in fracturing reconstruction of oil and gas reservoirs. Pipes are usually used as fracturing channels. Fracturing fluid inside of a pipe has the characteristic of high pressure and high velocity in fracturing process. Pump-starting and pump-stopping make the boundary conditions of the fracturing fluid

change in a short time, which give rise to water hammer phenomenon [1]. Water hammer effect changes the velocity and pressure of fracturing fluid inside of piping, which results in the vibration of piping. This may damage the piping or cause sealing failure of connections.

Housner and Feodos'ev analyzed the vibration of pinned–pinned horizontal pipe arising from the flow of the inner fluid. They found that the flow of the fluid influenced the frequencies of the pipe. There are coupled vibrations in the first few mode shapes [2, 3]. Zhang et al. [4] deduced the vibration equations of pipe in the axial direction and transverse direction and the flow equation of fluid with the consideration of fluid–solid interaction (FSI). Yang et al. [5] analyzed the pressure wave propagation from water hammer effect. Zhen Huang analyzed the vibration of piping in gas wells. He found that the velocity change in gas-induced erosion of piping. Vibration and erosion are the main sources of failure of piping in high pressure and high temperature (HPHT) wells [6]. Yihua Dou et al. analyzed the stress and deformation of conveying fluid pipe under axial force and inner fluid flow. They also discussed the influence of frequency of fluid on the amplitude of the pipe [7, 8]. Du et al. [9] analyzed the load, deformation, and stress of piping in fracturing process. Jun Zhu et al. analyzed the flow characteristics and the change in fluid considering the transient response of pipe in fracturing process. They also verified their results with experiments [10]. Li [11] established a model of equivalent axial force of piping considering the pressure arising from the flow of fluid inside and outside of piping. Yinping Cao et al. established a mechanical model of piping in a gas well. They found that the wellhead is the most dangerous place where the von Mises stress attains its maximum value. The stress inside of the piping is greater than the outside of the piping at the same cross section [12]. Fan et al. [13] established the FSI model in a gas well. They found the pressure buildup from shutting the well has a great effect on the axial vibration.

Existing research on water hammer mainly adopts analytic methods, numerical simulation, and experiments. They mostly focus on water hammer of fluid conveying pipe. For fracturing piping, especially SRV fracturing piping, a sudden change in pressure and velocity causes water hammer effect in the pump-starting and pump-stopping processes. It causes vibration of the piping, which may damage the piping or cause sealing failure of connections. One characteristic of water hammer of fracturing piping is its high pressure, which makes the variation of pressure larger. In this paper, the velocities and dynamic pressures of fracturing fluid as well as the axial velocities and additional stresses of piping at different depths in the pump-starting and pump-stopping processes are analyzed.

Establishment of the Differential Equations

The change in boundary conditions in pump-starting and pump-stopping breaks the original equilibrium state of the whole system. It causes water hammer and makes the flow parameters of fluid change with time. The continuity and motion equations of fracturing fluid inside piping are as follows:

$$\frac{\partial p}{\partial t}+v\frac{\partial p}{\partial x}+\rho c^2\frac{\partial v}{\partial x}+\frac{\lambda\rho v^2|v|}{2d}=0 \quad \text{(Eq 1)}$$

$$\frac{1}{\rho}\frac{\partial p}{\partial x}+\frac{\partial v}{\partial t}+v\frac{\partial v}{\partial x}+\frac{\lambda v|v|}{2d}=0 \quad \text{(Eq 2)}$$

Linearizing Eqs (1) and (2), the following equation set is obtained.

$$\begin{gathered}\left(\frac{\partial p}{\partial t}+v\frac{\partial p}{\partial x}+\rho c^2\frac{\partial v}{\partial x}+\frac{\lambda\rho v^2|v|}{2d_t}\right)+\zeta\left(\frac{1}{\rho}\frac{\partial p}{\partial x}+\frac{\partial v}{\partial t}+v\frac{\partial v}{\partial x}+\frac{\lambda v|v|}{2d}\right)=0\\ \left[\frac{\partial p}{\partial t}+\frac{\partial p}{\partial x}(v+\frac{\zeta}{\rho})\right]+\zeta\left[\frac{\partial v}{\partial t}+\frac{\partial v}{\partial x}\left(v+\frac{\rho c^2}{\zeta}\right)\right]+\frac{\lambda\rho v^2|v|}{2d}+\frac{\zeta\lambda v|v|}{2d}=0\end{gathered} \quad \text{(Eq 3)}$$

where p and v are the functions of x and t. The differential forms of p and v are as follows.

$$\begin{aligned}\frac{dp}{dt}&=\frac{\partial p}{\partial t}+\frac{\partial p}{\partial s}\frac{\partial s}{\partial t}\\ \frac{dv}{dt}&=\frac{\partial v}{\partial t}+\frac{\partial v}{\partial s}\frac{\partial s}{\partial t}\end{aligned} \quad \text{(Eq 4)}$$

Upward pressure and downward pressure are:

$$C^+:\begin{cases}\frac{dp}{dt}+\rho c\frac{dv}{dt}+\frac{\lambda\rho v^2|v|}{2d}+\frac{\rho c\lambda v|v|}{2d}=0\\ \frac{dx}{dt}=v+c\end{cases} \quad \text{(Eq 5)}$$

$$C^-:\begin{cases}\frac{dp}{dt}-\rho c\frac{dv}{dt}+\frac{\lambda\rho v^2|v|}{2d}-\frac{\rho c\lambda v|v|}{2d}=0\\ \frac{dx}{dt}=v-c\end{cases} \quad \text{(Eq 6)}$$

After simplification, the following equations are obtained.

$$C^+: p_i^j-p_{i-1}^{j-1}+\rho c\left(v_i^j-v_{i-1}^{j-1}\right)+\frac{\lambda c\rho}{2d}\left|v_{i-1}^{j-1}\right|v_{i-1}^{j-1}(\Delta x+v_{i-1}^{j-1}\Delta t)=0 \quad \text{(Eq 7)}$$

$$C^-: p_i^j-p_{i+1}^{j-1}-\rho c\left(v_i^j-v_{i+1}^{j-1}\right)-\frac{\lambda c\rho}{2d}\left|v_{i+1}^{j-1}\right|v_{i+1}^{j-1}\left(\Delta x-v_{i+1}^{j-1}\Delta t\right)=0 \quad \text{(Eq 8)}$$

Discretization of the Computational Domain

Figure 1 shows the discretization of the whole domain using characterized lines method. Time accuracy is $\Delta x/c$. Dimensional accuracy is L/n.

Integrating Eqs (7) and (8) along lines C^+ and C^-, the pressures at point E at time t are:

$$C^+ : p_{Ei} = M(C_P - Bv_{Ei}) \quad \text{(Eq 9)}$$

$$C^- : p_{Ei} = M(C_P + Bv_{Ei}) \quad \text{(Eq 10)}$$

The expressions of velocity v and pressure p are as follows.

$$p_{Ei} = (C_P + C_M)M/2 \quad \text{(Eq 11)}$$

$$v_{Ei} = (C_P - C_M)/(2B) \quad \text{(Eq 12)}$$

Definition of Boundary Conditions

Two cases of pressure change are included in this paper, i.e., sudden increase and sudden decrease. Sudden increase in pressure is caused by pump-starting, while sudden decrease in pressure is caused by pump-stopping.

Taking the fracturing piping between the wellhead and perforated section as the object, its length L is divided into N parts during the analysis. Plunger pump set is used during the fracturing process.

The flow rate of each pump is:

$$Q_s = \pm A_s r\omega(\sin\varphi + \lambda \sin 2\varphi/2) \quad \text{(Eq 13)}$$

Thus, the total fluid flow is $Q_t = \sum_{m=1}^{i} Q_s$. Q_s is positive when the phase angle is between 0 and π. Q_s is negative when the phase angle is between π and 2π.

The expression of flow rate in pump-starting is assumed as follows:

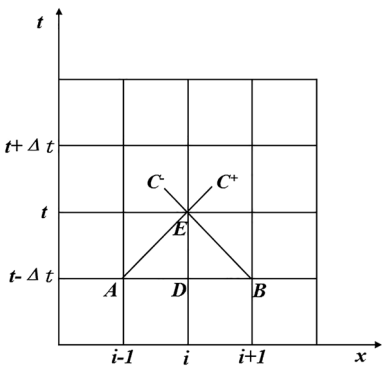

Fig. 1 Discretization of computational domain

$$Q = Q_0 + at^2 \quad \text{(Eq 14)}$$

In fracturing process, the pressure inside of piping is high. In pump-stopping, pressure is accumulated inside of the fracturing piping. The relationship of flow rate and pressure is:

$$\frac{v_1^j}{v_{\max}} = \tau\sqrt{\frac{p_1^j}{p_0}} \quad \text{(Eq 15)}$$

The expression of τ is:

$$\tau = \left(1 - \frac{t}{T}\right)^n \quad \text{(Eq 16)}$$

The expression of pressure with time is as follows.

$$p_1^j = \frac{\rho_t^2 a^2}{4}\left[-\frac{v_{\max}\tau}{\sqrt{p_0}} + \sqrt{\frac{v_{\max}^2\tau^2}{p_0} + \frac{4}{\rho_t a}v_N^{j-1} + \frac{4}{\rho_t^2 a^2}p_N^{j-1} - \frac{2\lambda\left|v_N^{j-1}\right|v_N^{j-1}}{\rho_t a^2 d_t}(\Delta x + v_N^{j-1}\Delta t)}\right]^2 \quad \text{(Eq 17)}$$

There is water hammer effect because impact loads are formed in the pump-stopping process. It makes the piping vibrate. When the vibration of piping is too violent, it may damage the piping.

Velocity of Fracturing Fluid in the Pump-Starting and Pump-Stopping Processes

Assuming the pump-starting time is 35 s, the velocities of fracturing fluid at the wellhead, depths of 2000 m, 4000 m, and 6000 m for the flow rates 2 m^3/min, 3 m^3/min, and 4 m^3/min are shown in Fig. 2. We can see that there is velocity fluctuation in the first 2 s. The reason is the pumps have not started completely. The velocity of fracturing fluid increases gradually with the increase in time. With the increase in depth, the time for the fracturing fluid reaching maximum value increases. The velocity increases faster for the greater flow rate at the same pump-starting time. The velocity increases with the increase in flow rate at the same depth. The increase is slower in the first 20 s. Obvious fluctuations of velocity of the fracturing fluid are observed after 20 s.

Water hammer effect in the pump-stopping process causes axial vibration of fracturing piping. Figure 3 shows the velocities of fracturing fluid at the wellhead, depths of 200 m, 300, and 400 m for the pump-stopping time of 15 s. It shows that the velocity of fracturing fluid deceases with fluctuation in the total pump-stopping time. The velocity decreases from 15 m/s at 0 s to 3.5 m/s at 14 s. It reaches to zero at 15 s because there is no flow of fracturing fluid.

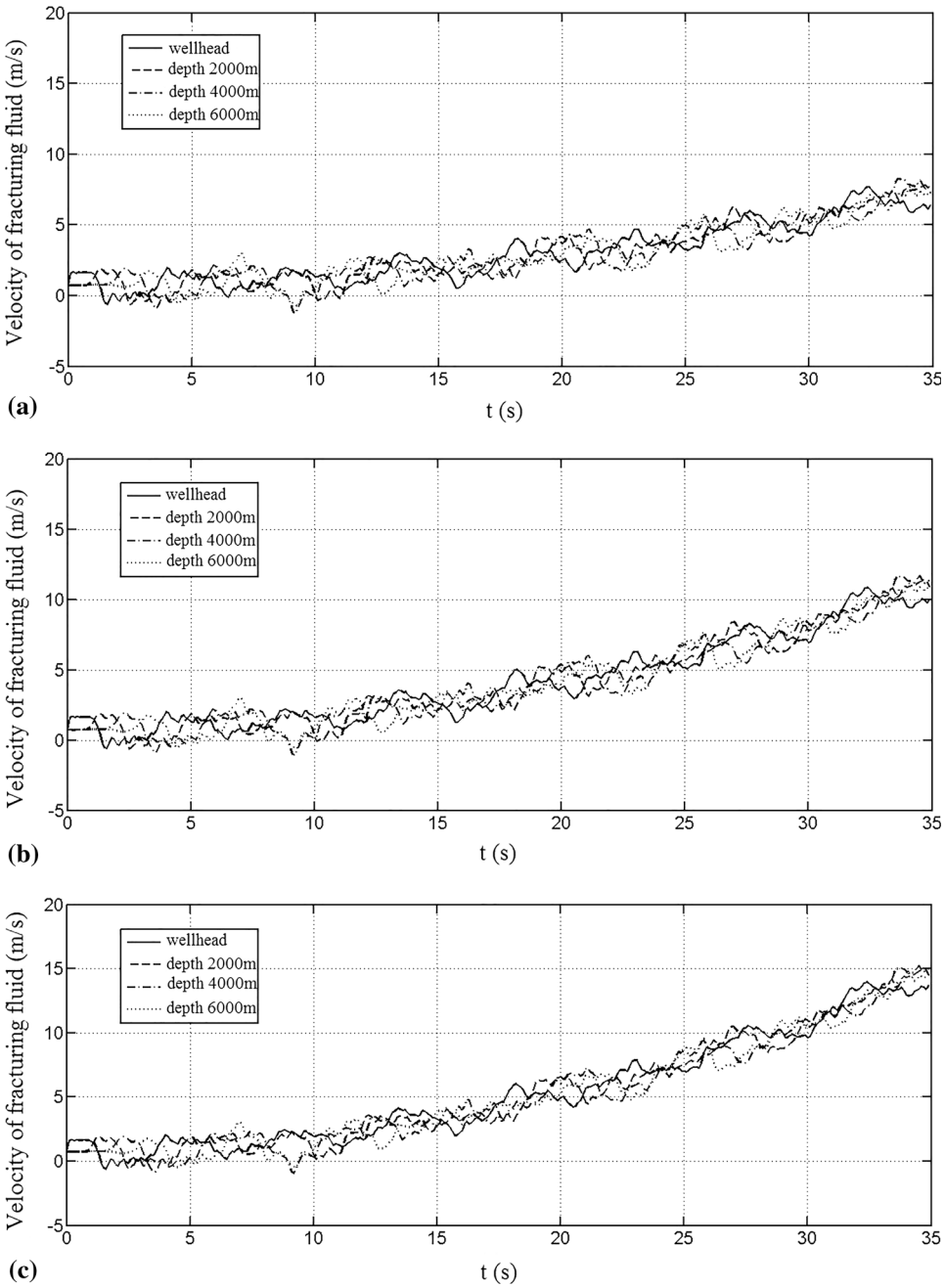

Fig. 2 Velocity of fracturing fluid in pump-starting process at a flow rate of (**a**) 2 m^3/min, (**b**) 3 m^3/min, and (**c**) 4 m^3/min

Dynamic Pressure of Fracturing Fluid in the Pump-Starting and Pump-Stopping Processes

Dynamic pressure of fracturing fluid changes when the flow rate of the fluid changes. Neglecting the static pressure, the dynamic pressure of fluid is expressed as ρv^2. The dynamic pressures of fracturing fluid in 35 s pump-starting time at the wellhead, depths of 2000 m, 4000 m, and 6000 m for the flow rates 2 m^3/min, 3 m^3/min, and 4 m^3/min are shown in Fig. 4. Similar to velocity of fracturing fluid, the dynamic pressure increases with fluctuation. In general, the dynamic pressure fluctuates most violently at the wellhead because of the transient pressure fluctuation from the rapid change in flow rate. Friction makes the fluctuations downhole less than the wellhead. With the increase in flow rate, the dynamic pressure increases obviously at the same depth. Because of wave propagation, there is no obvious periodic pressure change at first, but obvious increase in dynamic pressure is observed later. The maximum dynamic pressure is 1.28 MPa when the flow rate is 2 m^3/min, but reaches 1.80 MPa when the flow rate is 4 m^3/min.

Figure 5 shows the dynamic pressures of fracturing fluid at the wellhead, depths of 2000 m, 4000 m, and 6000 m for

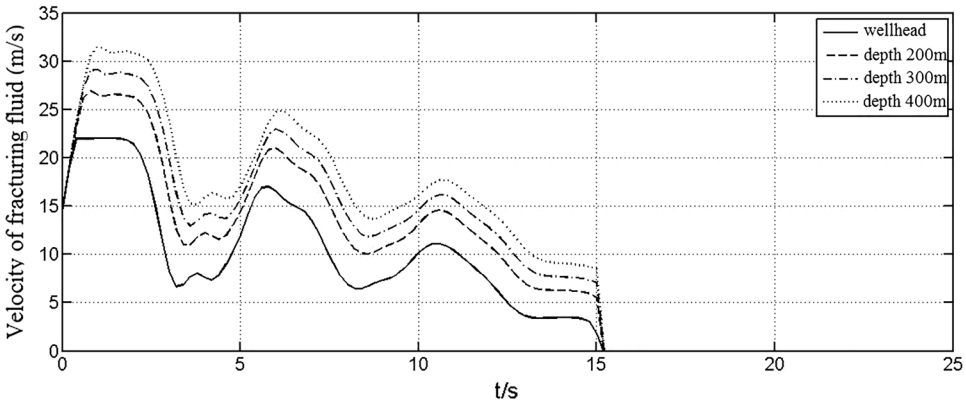

Fig. 3 Velocity of fracturing fluid in pump-stopping process

the pump-stopping time of 5 s, 10 s, and 15 s. In pump-stopping, the pump set gradually stops. There is a slight increase in dynamic pressure because some pumps still run. The increase rate of dynamic pressure at the wellhead is the greatest. Dynamic pressure is smaller with longer pump-stopping time. Shorter pump-stopping time makes greater dynamic pressure.

Axial Velocity of Fracturing Piping in the Pump-Starting and Pump-Stopping Processes

Axial velocity of fracturing piping has fluctuation because of the varied dynamic pressures. The axial velocity of fracturing piping in 35 s pump-starting time at the wellhead, depths of 2000 m, 4000 m, and 6000 m for the flow rates 2 m^3/min, 3 m^3/min, 4 m^3/min is shown in Fig. 6. It shows that the axial velocity of fracturing piping changes in a sinusoidal pattern, but its period is less than that of wave propagation. Because of the fluctuation of dynamic pressure, the axial velocity has positive and negative values. The velocity at the wellhead is obviously the greatest.

Figure 7 shows the axial velocity of fracturing piping at the wellhead, depths of 2000 m, 4000 m, and 6000 m for the pump-stopping time of 5 s, 10 s, and 15 s. The period of axial velocity is 4.8 s when pump-stopping time is 5 s. The maximum axial velocity is 4.9 m/s which decreases to 0.1 m/s at 25 s. The axial velocity decreases with depth. The maximum axial velocity is located at the wellhead. The shorter the pump-stopping time, the greater the axial velocity of fracturing piping.

Additional Axial Stress of Fracturing Piping in the Pump-Starting and Pump-Stopping Processes

Axial vibration is accompanied by transient loads. There is additional axial stress exerted on fracturing piping when there is axial vibration. The additional axial stresses of fracturing piping in 35 s pump-starting time at the wellhead, depths of 2000 m, 4000 m, and 6000 m for the flow rates 2 m^3/min, 3 m^3/min, 4 m^3/min are shown in Fig. 8. It shows that the additional axial stress increases with increased flow rate. The first increase in additional axial stress happens at depth 6000 m. The additional axial stress increases with depth. The additional axial stress at 6000 m has the maximum value and fluctuates most violently.

Figure 9 shows the additional axial stress of fracturing piping at the wellhead, depths of 2000 m, 4000 m, and 6000 m for the pump-stopping times of 5 s, 10 s, and 15 s. There are obvious fluctuation and vibration at the wellhead. Figure 9a shows that the maximum value is 415 MPa. The period is 4.8 s when pump-stopping time is 5 s. The additional axial stress decreases to 395 MPa at 25 s. Figure 9b shows that the maximum value is 390 MPa and decreases to 343 MPa at 25 s when pump-stopping time is 10 s. Figure 9c shows that the maximum value is 384 MPa and decreases to 275 MPa at 25 s when pump-stopping time is 15 s.

It is clear that longer pump-stopping time results in less additional axial stress. Similar to the pump-starting process, the additional stress at the wellhead is the greatest in the pump-stopping process. The additional axial stress in pump-stopping is greater than that in pump-starting. That

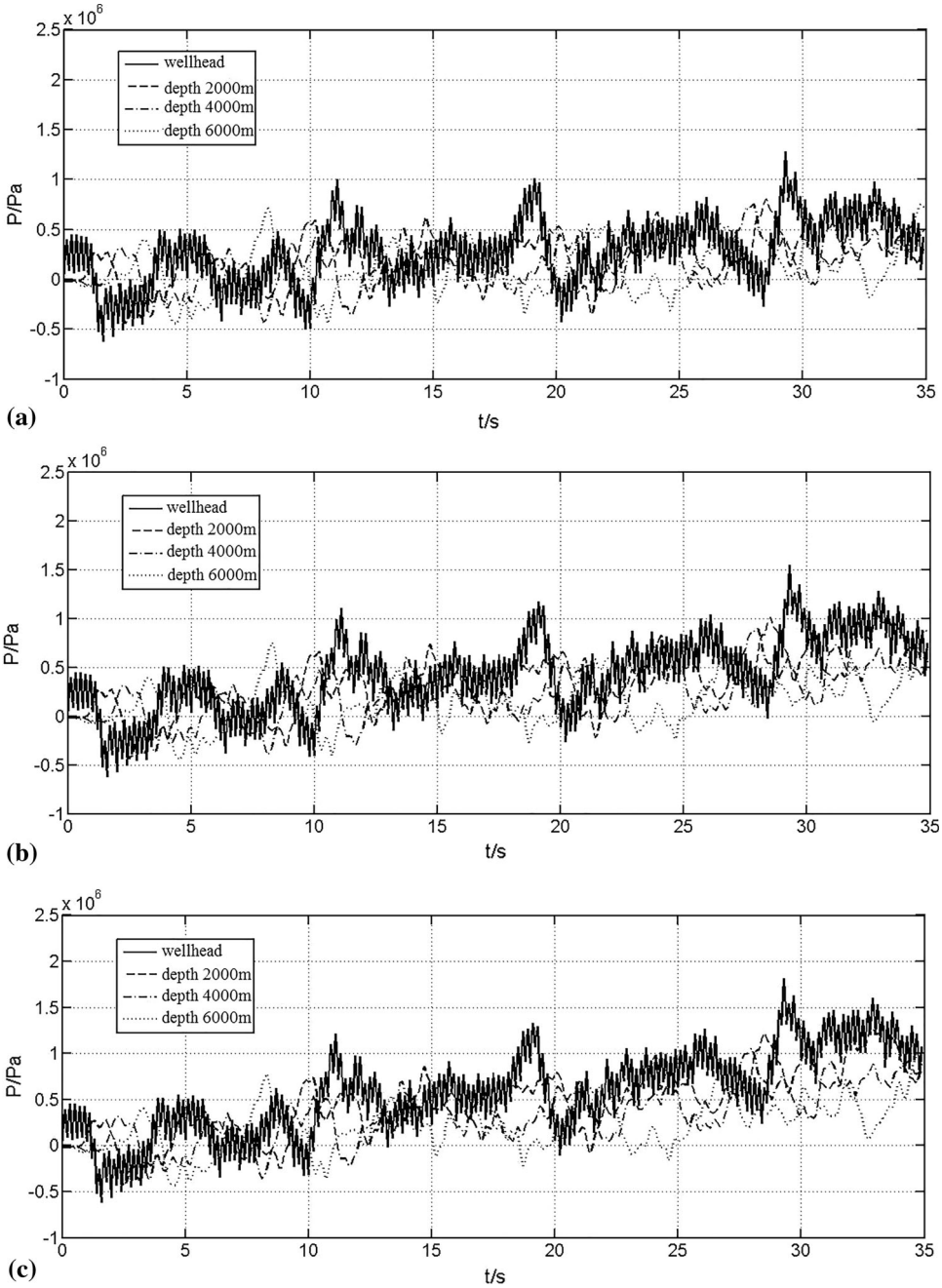

Fig. 4 Dynamic pressure of fracturing fluid in pump-starting process at a flow rate of (**a**) 2 m^3/min, (**b**) 3 m^3/min, and (**c**) 4 m^3/min

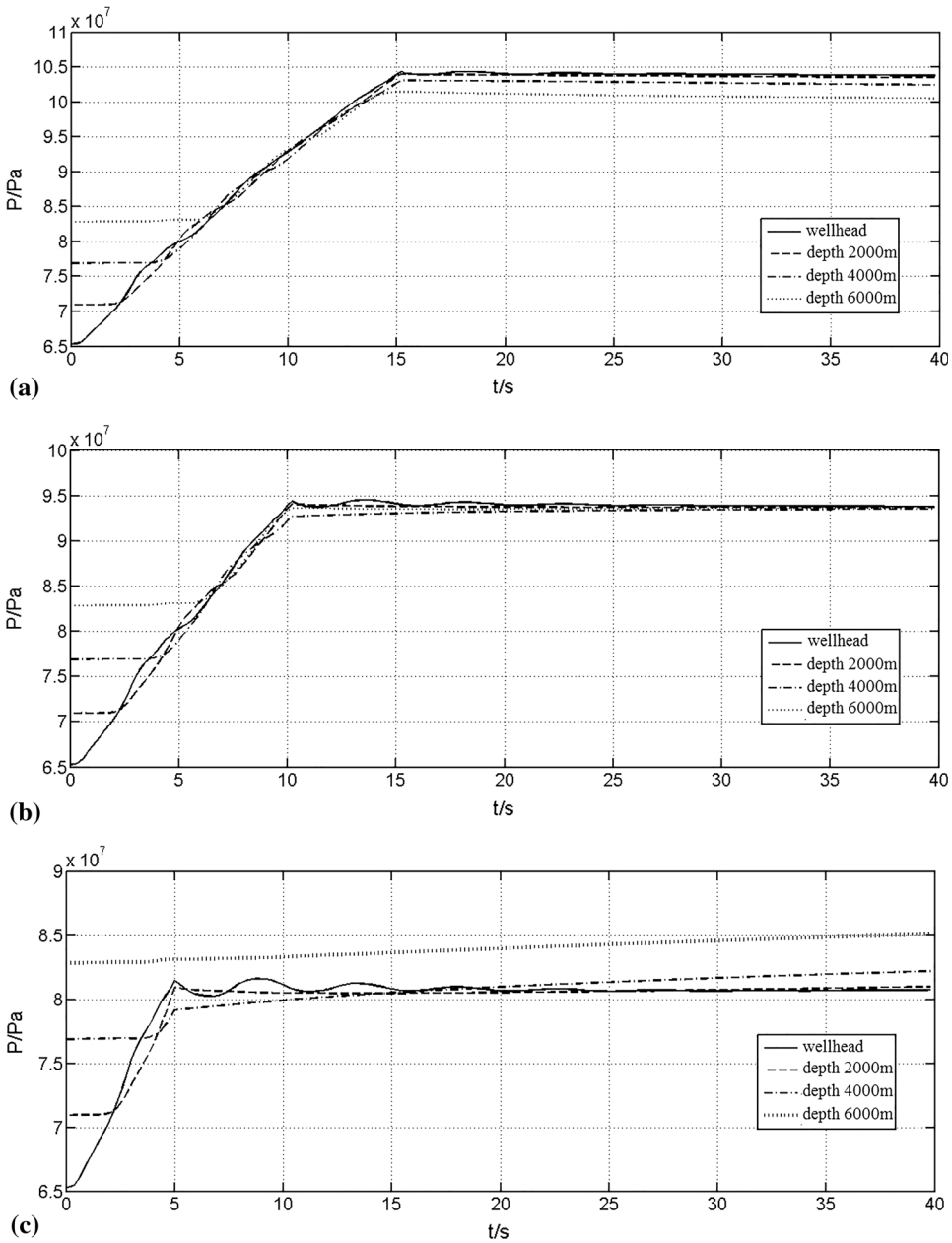

Fig. 5 Dynamic pressure of fracturing fluid in pump-stopping process with a pump-stopping time of (**a**) 5 s, (**b**) 10 s, and (**c**) 15 s

implies that piping maybe more easily be damaged in pump-stopping.

Conclusions

Characterized lines method was adopted to analyze the velocities and dynamic pressures of fracturing fluid, as well as the axial velocities and additional stresses of piping at different depths. Some conclusions are drawn from the above research.

1. Time for the increase in fracturing fluid velocity is longer for deeper position in the pump-starting process. The velocity of fracturing fluid increases when the flow rate increases. The velocity of fracturing fluid decreases with fluctuation in the pump-stopping process.
2. In pump-starting, dynamic pressure increases with fluctuation and is obviously greatest at the wellhead. With increased flow rate, dynamic pressure increases rapidly. In pump-stopping, the dynamic pressure decreases with small fluctuations. The increase in dynamic pressure is slower with longer pump-stopping time at the same depth.
3. In pump-starting, the axial velocity at the wellhead is obviously the greatest. In pump-stopping, the axial

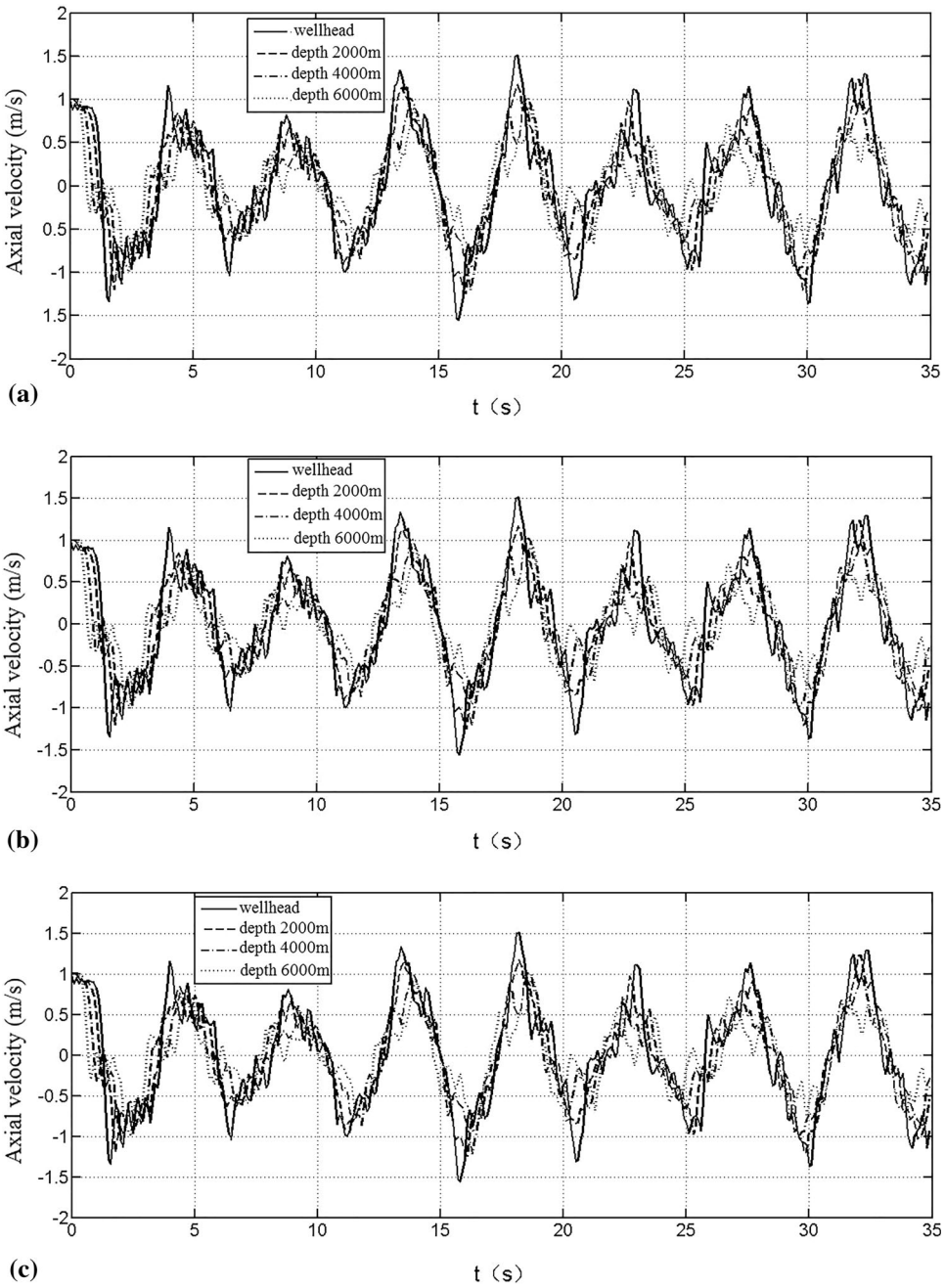

Fig. 6 Axial velocity of fracturing tubing in pump-starting process at a flow rate of (**a**) 2 m^3/min, (**b**) 3 m^3/min, and (**c**) 4 m^3/s

velocity decreases with increased depth. The velocity has the most violent fluctuation at the wellhead. The shorter the pump-stopping time is, the greater the axial velocity is.

4. In pump-starting, the additional axial stress increases with increased flow rate and depth. In pump-stopping, shorter time makes greater additional axial stress. Similar to the pump-starting process, the additional

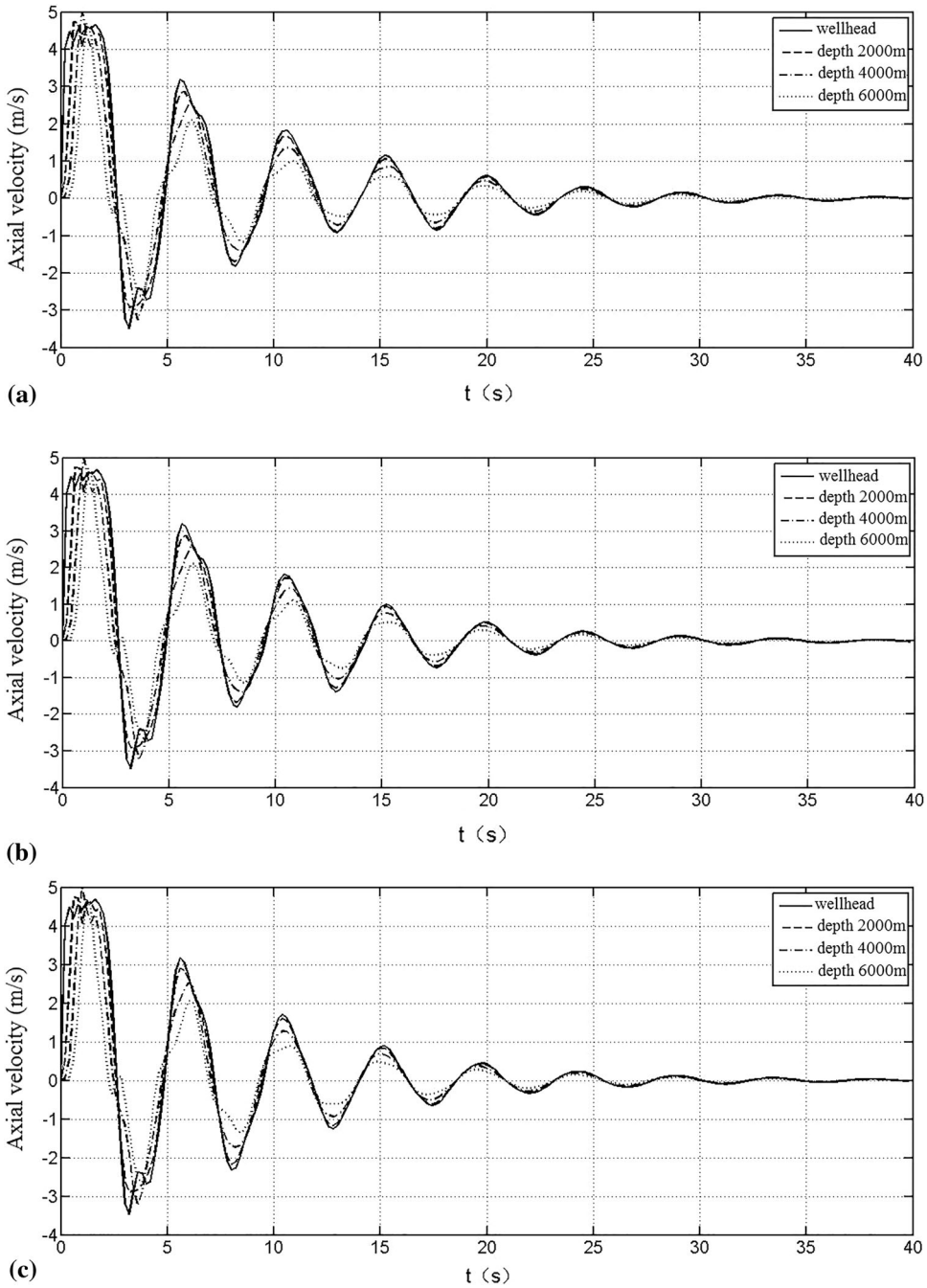

Fig. 7 Axial velocity of fracturing tubing in pump-stopping process with a pump-stopping time of (**a**) 5 s, (**b**) 10 s, and (**c**) 15 s

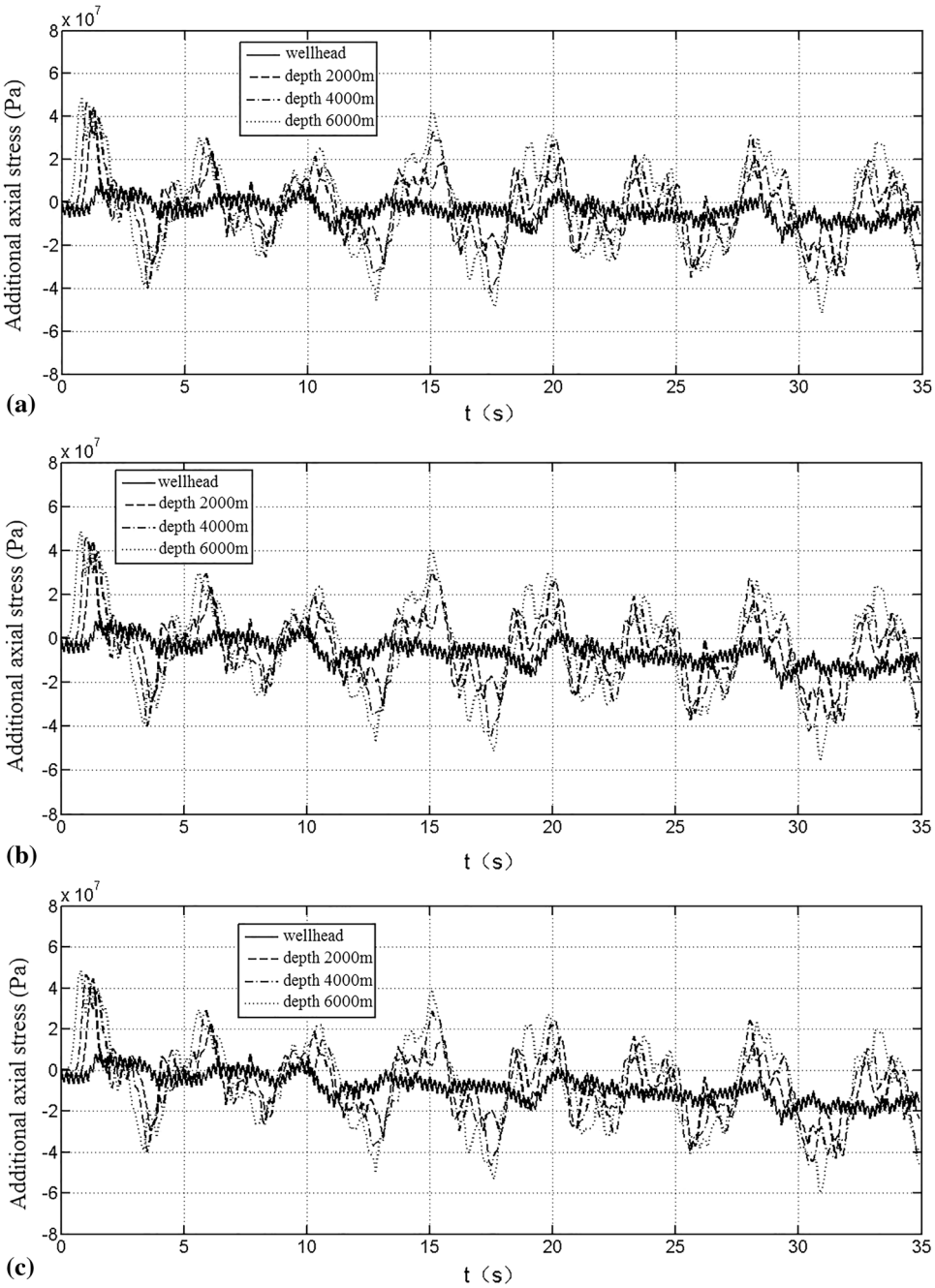

Fig. 8 Additional axial stress of fracturing tubing in pump-starting process at a flow rate of (**a**) 2 m^3/min, (**b**) 3 m^3/min, and (**c**) 4 m^3/min

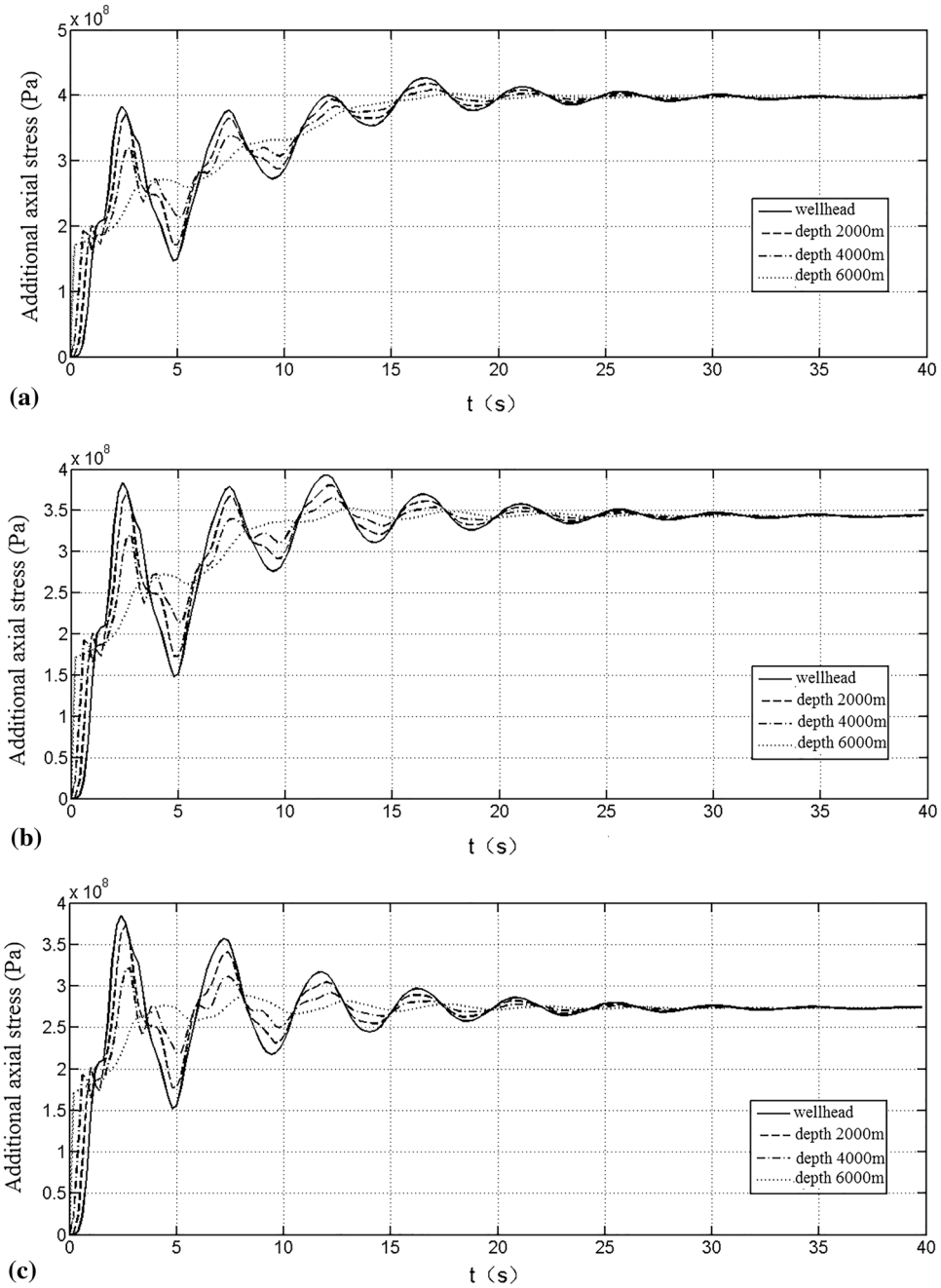

Fig. 9 Additional axial stress of fracturing tubing in pump-stopping process with a pump-stopping time of (**a**) 5 s, (**b**) 10 s, and (**c**) 15 s

axial stress is the greatest. The additional axial stress in the pump-stopping process is far greater than that in the pump-starting process, which will more likely damage the piping.

Acknowledgments This work was supported by the National Natural Science Foundation of China (Grant Nos. 51404198 and 51674199) and Important National Science and Technology Project (2016ZX05051003).

References

1. Z. Zhang, W. He, Analysis of factors affecting the time of closing the valve in the gravity pressure water transmission system. Sci. Technol. Eng. **13**(13), 3790–3792 (2013)
2. G.W. Housner, Bending vibration of pipeline containing flowing fluid. J. Appl. Mech. **19**, 205–208 (1952)
3. V.P. Feodod'ev, Vibrations and stability of a pipe when liquid flows through it. Inzhenernyi Sbornik **10**, 169–170 (1956)
4. L. Zhang, K. Yang, *Fluid–Solid Interaction and Its Application* (Science Press, Beijing, 2004), pp. 50–62
5. C. Yang, J. Zhang, Apparatus inducing water-hammer and the analysis and experiment of the water-hammer pressure wave propagation in the water system. Fluid Mach. **42**(9), 10–13 (2014)
6. Z. Huang, *The Research of Vibration Mechanism and Analysis of Dynamic Response of Tubing String* (Southwest Petroleum University, Chengdu, 2005)
7. Y. Dou, F. Zhang, Mechanics analysis of tubing and its application in high temperature high pressure and deep well. Drill. Prod. Technol. **30**(5), 17–20 (2007)
8. Y. Dou, K. Yu, X. Yang et al., Finite element analysis of fluid-structure interaction vibration of curved pipe. Mach. Des. Manuf. Eng. **46**(2), 18–21 (2017)
9. X. Du, H. Wang, S. Wang et al., Mechanics analysis of downhole string used for deep well fracturing and its application. Oil Field Equip. **8**(28), 28–33 (2008)
10. J. Zhu, H. Wong, D. Li et al., Study on fracturing fluid characteristics based on fluid-solid coupling technology. Oil Field Equip. **39**(3), 1–5 (2010)
11. Z. Li, Influence of internal and external pressure on equivalent axis force and stability of pipe string in oil wells. J. China Univ. Pet. **2**(1), 31–35 (2011)
12. Y. Cao, G. Tang, C. Tang et al., An analysis of the stress strength of vibration gas recovery pipestring. China Pet. Mach. **40**(3), 80–82 (2012)
13. H. Fan, Y. Wang, L. Zhang et al., A fluid-solid coupled oscillation model for completion string and its application in high pressure gas well. ACTA Pet. Sin. **32**(3), 547–550 (2011)